Journal Pre-proofs

Parametric study on melting process of a shell-and-tube latent thermal energy storage under fluctuating thermal conditions

Zhi Li, Yiji Lu, Rui Huang, Lei Wang, Ruicheng Jiang, Xiaonan Yu, Xiaoli Yu

Please cite this article as: Z. Li, Y. Lu, R. Huang, L. Wang, R. Jiang, X. Yu, X. Yu, Parametric study on melting process of a shell-and-tube latent thermal energy storage under fluctuating thermal conditions, *Applied Thermal Engineering* (2020), doi: https://doi.org/10.1016/j.applthermaleng.2020.115898

This is a PDF file of an article that has undergone enhancements after acceptance, such as the addition of a cover page and metadata, and formatting for readability, but it is not yet the definitive version of record. This version will undergo additional copyediting, typesetting and review before it is published in its final form, but we are providing this version to give early visibility of the article. Please note that, during the production process, errors may be discovered which could affect the content, and all legal disclaimers that apply to the journal pertain.
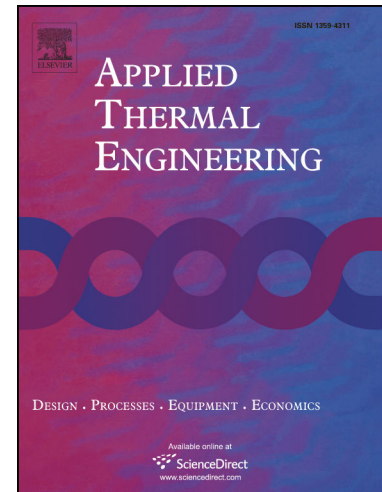
Parametric study on melting process of a shell-and-tube latent thermal energy storage under fluctuating thermal conditions

Zhi Li [a,b], Yiji Lu [a,c,]*, Rui Huang [a,b,]*, Lei Wang [a,d], Ruicheng Jiang [a], Xiaonan Yu [a], Xiaoli Yu [a,b]

[a] *Department of Energy Engineering, Zhejiang University, Hangzhou, 310027, China*

[b] *Ningbo Research Institute, Zhejiang University, Ningbo, 315100, China*

[c] *Durham Energy Institute, Durham University, Durham, DH1 3LE, United Kingdom*

[d] *Ningbo C.S.I Power & Machinery Group Co., Ltd., Ningbo, 315020, China*

Abstract

The intermittent and fluctuating nature of thermal sources such as solar, geothermal, industrial processes and waste heat from internal combustion engines is one of the most challenging research areas and currently limits the implementation of heat recovery systems such as Organic Rankine Cycle (ORC) technology. Latent Thermal Energy Storage (LTES) using Phase Change Material (PCM) is a promising solution to mitigate fluctuations of thermal sources and maintaining the heat recovery systems under designed conditions. However, the melting process significantly affects the energy storage performance, as well as the design and optimisation of the LTES system under fluctuating thermal conditions. In this study, the melting process of a shell-and-tube LTES unit, under a sinusoidal heat source, is numerically investigated in order to consider the effects of period and amplitude. Then, the effects of PCM thermal conductivity, with and without nanoparticles, were simulated and the heat transfer coefficient of sinusoidal heat source on the melting process is separately analysed under the sinusoidal heat source condition. The parametric study of thermal conductivity and heat transfer coefficient is conducted to evaluate whether these parameters affect the period and amplitude of sinusoidal heat sources on the melting process of LTES. The results indicate an overall trend of the total melting time and heat storage capacity of LTES decreasing whilst there is an increase of period and amplitude of the fluctuating heat source.

Keywords: Fluctuating thermal source, Latent thermal energy storage, Period and amplitude, Shell-and-tube heat exchanger, Phase change material

Email address: luyiji0620@gmail.com (Y. Lu); hrss@zju.edu.cn (R. Huang);

Nomenclature	
A	The fluctuating amplitude of heat source (K)
$c_{p,f}$	The specific capacity of heat transfer fluid (J/kg K)
$c_{p,p}$	The specific capacity of phase change material (J/kg K)
f	Liquid volume fraction
H	The total enthalpy of phase change material (J/kg)
h	The sensible heat of PCM (J/kg)
h_f	Heat transfer coefficient of fluctuating heat source (W/m^2 K)
L	The latent heat of PCM (J/kg)
P	Fluctuating period of the heat source (s)
r_1	Radium of inner tube (m)
r_2	Radium of outer tube (m)
T_m	Melting temperature of PCM (K)
Greek letters	
α	Thermal expansion coefficient (K^{-1})
λ	Thermal conductivity (W/m K)
μ	Dynamic viscosity (Pa s)
ρ	Density (kg/m^3)

1. Introduction

To tackle climate change issues, timely research on the delivery of sustainable energy solutions is critical, resulting in the reduction of emissions, reduced costs for industries through the technological development of improved thermal energy and utilisation energy systems, and support a stable energy security position. The key research challenge in thermal energy engineering is how to overcome the intermittent and fluctuating nature of thermal sources such as solar, industrial waste heat and geothermal energy [1, 2]. To achieve an efficient and effective thermal energy system, the adoption of thermal energy storage is essential. The integration and utilisation of Latent Thermal Energy Storage (LTES) [3] with heat recovery technologies such as Organic Rankine Cycle (ORC) technology [4, 5] offers the most potential, cost-effective solution and has been widely investigated worldwide. The LTES using Phase Change Material (PCM) to form the thermal energy system can be used as a buffer to overcome thermal fluctuations and benefits from the high latent heat and constant phase change temperature of the selected PCM [6, 7]. LTES stores the fluctuating thermal sources and maintains the heat recovery system within the designed conditions [8, 9] optimising the performance of the thermal energy conversion system.

Such a system has been widely investigated for solar power plants and industrial waste heat recovery to overcome and balance the instability of solar radiation and fluctuations of industrial heat sources. For example, Hassan and Rouhollah [10] investigated the dynamic performance of a solar power plant assisted with an LTES system. The results indicated that the solar fraction of the combined system was enhanced by 90.5% in comparison with the solar power plant without an LTES system. Jacob *et al.* [11] conducted a comparative study on several thermal energy storage systems for concentrated solar power plants considering both economic and environmental effects. It was found that the encapsulated PCM (EPCM) system had the smallest embodied energy while the two-tank molten salt achieved the maximum embodied energy. Li *et al.* [12] analysed the dynamic performance of a solar ORC system integrating with LTES due to the intermittent thermal souce conditions. Results demonstrated that the introduction of LTES reduced the

instability of solar radiation and improved the matching performance of end-user demands in small-scale solar ORC systems and domestic-scale solar heating system. Gioacchino *et al.* [13] proposed a newly developed PCM-based heat recovery system to reduce the variability of off-gas temperatures and thermal power fluctuation in the steel industry. It was found that the high recovery efficiency, low investment and operation cost can be achieved by using the PCM-based technology. The authors [14] proposed and investigated a heat recovery system for the engine waste heat recovery, integrating LTES with ORC technology concuting a comparative studying the system performance with twelve PCMs under different heat source conditions. Results indicated the $LiNO_3$-KCl-$NaNO_3$ is the optimal candidate to be used as it achieved the best performance among the selected PCMs.

The studies described above have demonstrated the feasibility and superiority of heat recovery systems integrating with LTES to address the fluctuation of solar radiation and industrial heat sources. However, all of these studies largely focused on the overall system performance without considering the detailed melting process of PCM, and the studies main perspective was thermodynamicas or consideration of the PCM as a heat capacity. The analysis and optimisation of the PCM melting process are important for improving the energy storage performance of LTES under the steady heat source, which has been widely considered in previous studies. Li and Wu [15] numerically investigated the charging-discharging performance of a shell-and-tube LTES unit, considering the effects of HTF, PCM and fins. The results concluded that both the total melting time and solidification time was shortened at least 14%, benefiting from the utilisation of the extended fins and the composite PCM. Tao *et al.* [16] evaluated the effects of the PCM thermophysical properties on the charging performance of a high-temperature LTES unit. Other studies have concentrated on the heat transfer enhancement and heat exchanger design of LTES systems. Han *et al.* [17] conducted a comparative study to determine the effects of horizontal and vertical shell-and-tube models with different inlet conditions of heat transfer fluid including the effects of natural convection. Results showed that the natural convection caused a non-uniform distribution of the solid-liquid interface, which sped up the melting process. Wang *et al.* [18] carried out a numerical

study to analyse the melting process of shell-and-tube LTES under different geometrical parameters of fins, including fin length, fin ratio and fin angle. Due to the lower thermal conductivity of the majority of PCM, a large number of studies have focused on thermal conductivity enhancement and heat transfer enhancement of LTES, such as heat pipes [19], nanoscale additives [20], porous media [21] and cascaded PCM [22].

The majority of the present studies on shell-and-tube LTES systems were conducted based on steady thermal boundary conditions and inlet conditions. In a small number of studies, the fluctuation heat source was studied but without consideration of the detailed heat transfer process of PCM under fluctuating thermal boundaries. Instead, most of the related studies conducted computations from a perspective of thermodynamics or considering the PCM as a large heat capacity. However, the fluctuation of inlet temperature or mass flow rate should be considered in the design stage of LTES systems used for recovering industrial waste heat [2]. Some researchers have noticed this challenge. Tao *et al.* [23] numerically studied the charging performance of a shell-and-tube LTES under unsteady inlet temperature and mass flow rate with a linear variation. The results indicated that a greater initial inlet temperature and mass flow rate could substantially reduce the melting time of the paraffin LTES. Xu *et al.* [24] optimised the thermal performance of a cascaded shell-and-tube LTES system with a quadratic-variation inlet temperature of HTF from the aspect of exergy, entropy and entransy analysis. The results showed that the optimal thermal performance of the steady case was better than that of the fluctuating case. Huo *et al.* [25] investigated the effects of the time-dependent intermittent heat flux on the energy storage performance aiming to increase the energy storage density and reduce the final average temperature of a solar LTES tank. The proposed transient heat flux has the characteristic of the square wave and its period and amplification were numerically evaluated. The results proved that the time-dependent heat flux could reduce the final average temperature but increase the total melting time compared to the constant heat flux. The authors recently reported a comparative study focusing on the melting process of a shell-and-tube LTES under constant and sinusoidal inlet temperature [26]. The results indicated the sinusoidal condition resulted in shorter total melting time but smaller energy

storage capacity with the increase of period and amplitude compared with the constant condition and the same charging time. This study revealed the difference of the effects of constant and sinusoidal inlet temperature on the melting process of shell-and-tube LTES, as well as demonstrating the importance of revealing the melting process of shell-and-tube LTES under fluctuating thermal boundary conditions.

In summary, it can be concluded that the melting process of shell-and-tube LTES under sinusoidal heat source requires further research to better understand the melting process of LTES under fluctuating thermal conditions for the future design and optimisation of LTES heat exchanger for heat recovery applications. Specifically, the comprehensive investigation of the effects of different periods and amplitudes, which significantly affects the energy storage performance as well as the design and optimisation of LTES should be conducted. Furthermore, there is also a lack of knowledge about the effects of PCM thermal conductivity and heat transfer coefficients of fluctuating heat sources on the melting process of LTES. In this study, the characteristics of fluctuating heat sources are modelled as a sinusoidal function with different periods and amplitudes, and the melting process of a shell-and-tube LTES under fluctuating heat source is comprehensively investigated based on a 2D simulation model. Other crucial parameters including PCM thermal conductivity and heat transfer coefficient of fluctuating heat source are analysed on the melting process of LTES, aiming to reveal how the fluctuating heat sources with different periods and amplitudes affect the melting process of shell-and-tube LTES and its energy storage performance.

2. Model description

2.1 Physical model

The schematic diagram of the shell-and-tube LTES heat exchanger is depicted in **Fig. 1**. The length of the LTES heat exchanger is 1000 mm, and the radius of the inner tube and outer shell are 12.5 mm and 25 mm respectively. Along the flow direction of Heat Transfer Fluid (HTF), each A-A section of PCM is heated by the fluctuating heat source and a

6

similar heat transfer process is undertaken. Therefore, a two-dimensional A-A section of LTES has been selected as the

research objective. The following assumptions are adopted to simplify the physical model and the computational

modelling.

(1) The thermophysical properties of PCM are independent of temperature.

(2) The flow in the liquid PCM is assumed to be Newtonian laminar and incompressible.

(3) The thermal resistance of the inner wall is neglected while the outer wall of the LTES is adiabatic.
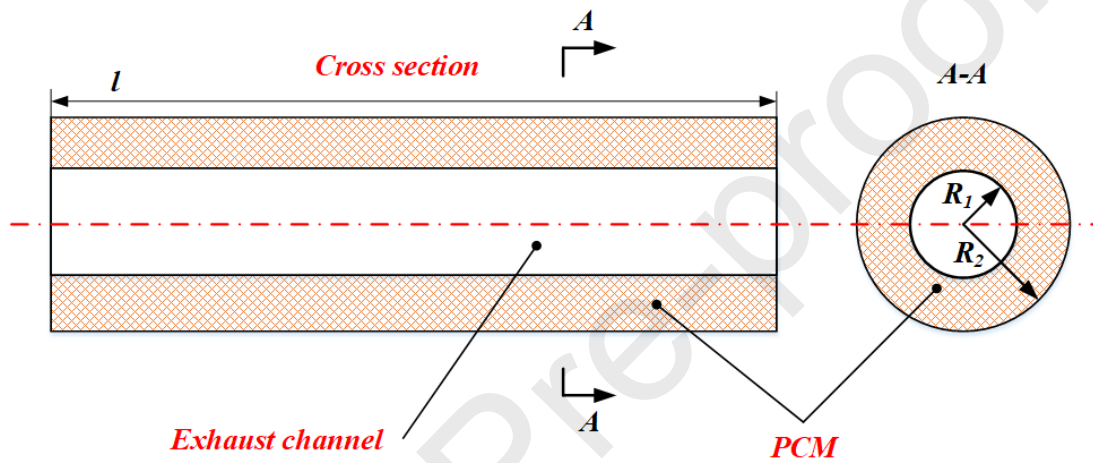
Fig. 1. Schematic diagram of the latent thermal energy storage evaporator.

2.2 Thermophysical properties of PCM with nanoparticle

The thermal conductivity of PCM is an important of the charging process. To evaluate the effects of thermal conductivity

on the charging performance of shell-and-tube LTES under fluctuating heat source, Al_2O_3 nanoparticles are added into

the inorganic salt to form nano-PCM, which can substantially improve the thermal conductivity of PCM. After adding

nanoparticles into the pure PCM, the thermophysical properties have been changed and they need to be calculated in

accordance with the volume fraction of nanoparticles. The simple mixture method [27, 28] is used to calculate the

thermophysical properties of the nano-PCM. It should be noted that the simple mixture model only considered the

promotion effects of thermal conductivity of PCM due to the addition of nano-particles but neglected the possible

settling effects of nano-particles. This is because one of the aims in this study is to evaluate the effects of PCM thermal

conductivity on the melting process of LHES under sinusoidal heat sources. The calculation for the density, specific

capacity, latent heat and thermal expansion coefficient are described as follows [27]:

$$\rho_{npcm} = \left(1 - \phi_{np}\right)\rho_{pcm} + \phi_{np}\rho_{np} \tag{1}$$

$$\left(\rho c_p\right)_{npcm} = \left(1 - \phi_{np}\right)\left(\rho c_p\right)_{pcm} + \phi_{np}\left(\rho c_p\right)_{np} \tag{2}$$

$$\left(\rho L\right)_{npcm} = \left(1 - \phi_{np}\right)\left(\rho L\right)_{pcm} \tag{3}$$

$$\left(\rho\beta\right)_{npcm} = \left(1 - \phi_{np}\right)\left(\rho\beta\right)_{pcm} + \phi_{np}\left(\rho\beta\right)_{np} \tag{4}$$

The thermal conductivity and dynamic viscosity are the critical parameters which influence the charging process of

PCM. The thermal conductivity of nano-PCM is calculated by the equation proposed by Vajjha and Das [29]:

$$k_0 = k_{pcm}\frac{k_{np} + 2k_{pcm} - 2\phi\left(k_{pcm} - k_{np}\right)}{k_{np} + 2k_{pcm} + \phi\left(k_{pcm} - k_{np}\right)} \tag{5}$$

$$k_d = 5\times10^4 \beta_k \phi\left(\rho C_p\right)_{pcm}\sqrt{\frac{B_0 T}{\rho_n d_p}}f\left(T,\phi\right) \tag{6}$$

$$f\left(T,\phi\right) = \left(2.822\times10^{-2}\phi + 3.917\times10^{-3}\right)\frac{T}{T_{ref}} - \left(3.067\times10^{-2}\phi + 3.911\times10^{-3}\right) \tag{7}$$

$$k_{npcm} = k_0 + k_d \tag{8}$$

The effective dynamic viscosity of the nano-PCM is given by the Brinkman equation [30]:

$$\mu_{npcm} = \frac{\mu_{pcm}}{\left(1 - \phi\right)^{2.5}} \tag{9}$$

The thermophysical properties of the selected PCM and nanoparticles are listed in **Table 1**.

Table 1 Thermophysical properties of the PCM candidates analsed in this study

Parameters	PCM (LiNO$_3$-NaNO$_3$-KCl) [3]	Al$_2$O$_3$ nanoparticle [30]	Composite PCM with 5% Al$_2$O$_3$
ρ (kg/s)	2297	3980	2381

λ (W/m·K)	0.58	58.49	1.26
c_p (J/kg K)	1330	778	1284
μ (Pa s)	0.003	n.a.	0.0034
T_m (K)	433	n.a.	433
ΔH (kJ/kg)	266	n.a.	243.8
α (K^{-1})	4e-4	1.67e-5	3.67e-4

2.3 Governing equations

In this section, a two-dimensional transient heat transfer model for the cross-section of LTES based on the enthalpy method will be presented to simulate the moving boundary problem within the PCM. The continuity equation for PCM is written as follows:

$$\frac{\partial \rho}{\partial t} + \frac{\partial (\rho u)}{\partial x} + \frac{\partial (\rho v)}{\partial y} = 0 \tag{10}$$

In the enthalpy method, the energy equations for liquid state and solid state have the same form. The solid-liquid interface is indicated as a mushy zone to separate the two phases. The energy equation for PCM is described as follows:

$$\frac{\partial \rho H}{\partial t} + \frac{\partial (\rho u H)}{\partial x} + \frac{\partial (\rho v H)}{\partial y} = \frac{\partial}{\partial x}\left(k \frac{\partial T}{\partial x} \right) + \frac{\partial}{\partial y}\left(k \frac{\partial T}{\partial y} \right) \tag{11}$$

Where H represents the total enthalpy of sensible enthalpy and latent enthalpy, which can be calculated by equation (3) and (4). h_{ref} denotes the sensible enthalpy at the reference temperature T_{ref}.

$$H = h + f \cdot L \tag{12}$$

$$h = h_{ref} + \int_{T_{ref}}^{T} c_p dT \tag{13}$$

Where f refers to the liquid volume fraction calculated by equation (5). It should be noted that the liquid volume fraction

9

lies between 0~1 in the mushy zone.

$$
f = \begin{cases} 0 & T < T_{solidus} \\ \dfrac{T - T_{solidus}}{T_{liquidus} - T_{solidus}} & T_{solidus} \le T \le T_{liquidus} \\ f = 1 & T > T_{liquidus} \end{cases} \tag{14}
$$

Substituting equation (3) -(5) into equation (2), the energy equation can be written as:

$$
\frac{\partial \rho h}{\partial t} + \nabla \cdot \left(\rho v h \right) = \nabla \cdot \left(k \nabla T \right) - \frac{\partial \rho fL}{\partial t} - \nabla \cdot \left(\rho v fL \right) \tag{15}
$$

The natural convection has a significant impact in accelerating the melting process of LTES [31]. Due to the small

variation in density, the natural convection is taken into consideration via the Boussinesq approximation [32]:

$$
\left(\rho - \rho_0 \right) g = -\rho_0 \beta \left(T - T_0 \right) \tag{16}
$$

Then the momentum equation considering natural convection for PCM has a form as follows:

$$
\frac{\partial \left(\rho u \right)}{\partial t} + \frac{\partial \left(\rho uu \right)}{\partial x} + \frac{\partial \left(\rho uv \right)}{\partial x} = -\frac{\partial p}{\partial x} + \frac{\partial}{\partial x}\left(\mu \frac{\partial u}{\partial x} \right) + \frac{\partial}{\partial y}\left(\mu \frac{\partial u}{\partial y} \right) + A_{mush} u \tag{17}
$$

$$
\frac{\partial \left(\rho v \right)}{\partial t} + \frac{\partial \left(\rho uv \right)}{\partial x} + \frac{\partial \left(\rho vv \right)}{\partial x} = -\frac{\partial p}{\partial y} + \frac{\partial}{\partial x}\left(\mu \frac{\partial v}{\partial x} \right) + \frac{\partial}{\partial y}\left(\mu \frac{\partial v}{\partial y} \right) + A_{mush} v + \rho g \alpha \left(T - T_m \right) \tag{18}
$$

In equation (9), the parameter A_{mush} is a constant to describe how fast the velocity is decreased to zero when the PCM

solidifies, which is calculated by [33]:

$$
A_{mush} = -C \frac{\left(1 - f \right)^2}{f^3 + \varepsilon} \tag{19}
$$

The constant ε is a very small number to prevent the division by zero. The computation is conducted by the software

Ansys/Fluent 14.5.

10

2.4 Model of fluctuating heat source
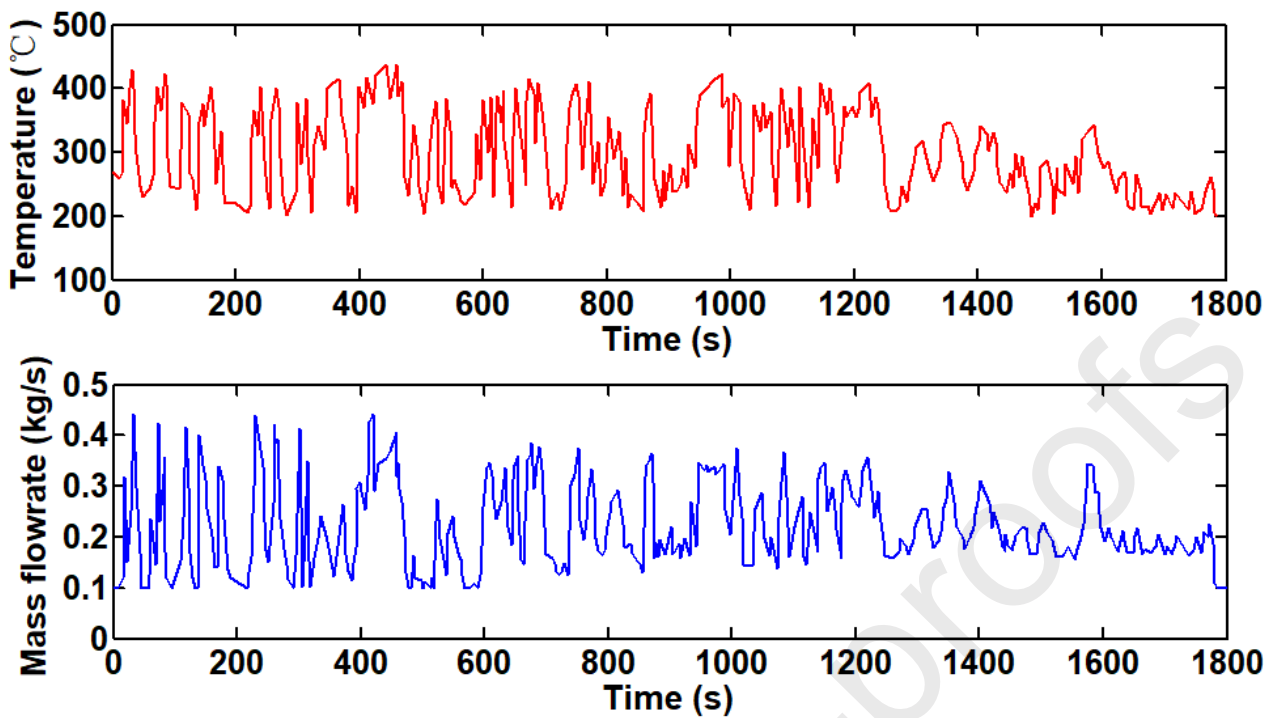
Fig. 2. Temperature and mass flowrate profiles of engine exhaust under the European Transient Cycle [14].

The temperature of different heat sources can fluctuate in different periods varying from minutes (even seconds) to hours, as well as with different amplitudes. The period and amplitude are important indicators and represent the characteristics of different fluctuating heat sources. To reveal how a fluctuating heat source affects the heat transfer process of the shell-and-tube LTES, the effects of periods and amplitudes for a fluctuating heat source need to be considered. **Fig. 2** shows an example of fluctuating conditions from engine exhaust heat. It can be seen that the temperature and mass flow rate profiles are quite complex. Other heat sources such as exhaust gas in industrial processes have similar fluctuating conditions as reported in the Ref. [2]. To make the heat transfer analysis symmetrical, the profiles can be analysed and desconstructed in order to extract the different components of fluctuation by using Discrete Fourier Analysis. Both the mass flow rate and temperature profiles can be seen as an irregular function or time series that can be decomposed into a sum of sinusoids of different frequencies [34, 35].

To idenify the fundamental laws associated with the charging process of shell-and-tube LTES under fluctuating heat

11

source, the fluctuating heat source is modeled as a series of sinusoidal functions with different periods and amplitudes.

In this study, the inlet temperature of the periodic heat source is described as a sinusoidal function in the following

equation:

$$T_{HTF} = a \cdot \sin(\pi t / b) + 573 \tag{20}$$

Where a and b are coefficients to determine the period and amplitude of the fluctuating heat source. In this study, the

periods of fluctuating heat source are considered as P= [1, 5, 10, 15, 30, 60] minutes, while the amplitude changes within

the range of A= [20, 40, 60, 80, 100] K.

2.5 Initial and boundary conditions

The initial conditions for PCM:

$$T_{PCM}(x, y) = T_0 \tag{21}$$

The boundary condition for HTF is:

$$T_{HTF,in} = T_{HTF} \tag{22}$$

The boundary condition for the outer wall is:

$$\frac{\partial T_{PCM}}{\partial r}(r = r_2) = 0 \tag{23}$$

The boundary condition for the inner wall is:

$$h_{HTF}(T_{HTF} - T_{PCM}) = -k \frac{\partial T_{PCM}}{\partial r}(r = r_1) \tag{24}$$

3. Independency study and model validation

Before the simulation, the variation of grid size and time step was studied. The computational domain is a two-

dimensional grid and is created in three different sizes of 0.5 mm, 0.8 mm and 1 mm. Different time steps including 0.5

s, 1 s, 2 s and 5 s are also assessed to ensure the selected time step does not affect the computational results. **Fig. 3**

shows the results of time step and grid size verification, therefore, the grid size of 0.8 mm and the time step of 1 s are

selected in the following simulations.
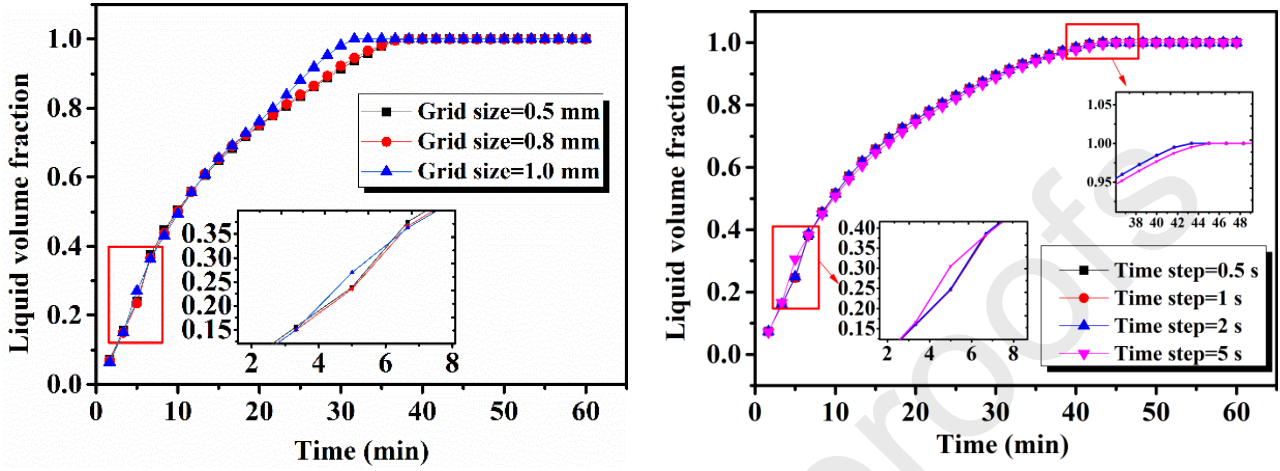
Fig. 3. Validation of the computational time step and grid size. (a) grid size. (b) time step.

To validate the soundness and reliability of the numerical model adopted in this research, a comparison between the

present simulation results and experimental work in reference [36] is conducted using the same geometry size and

operating conditions. In the experimental setup, two thermocouples were placed inside the PCM with the coordinates of

(x= 0.95 m, r= 0.001 m) and (x= 0.51 m, r= 0.002 m). The inlet temperature of HTF was set at 310.7 K. The comparative

results are described in **Fig. 4**. It can be seen that the reported temperature in the present simulation closely aligns with

the experimental data in reference [36]. The error analysis indicated the maximum error between the present simulation

results and experimental data in Refs. [36] is 4.67%, and the reason is due to the neglecting the outer wall and the natural

convection of the air. The close agreement proves the reliability and correction of the adopted numerical model.

13
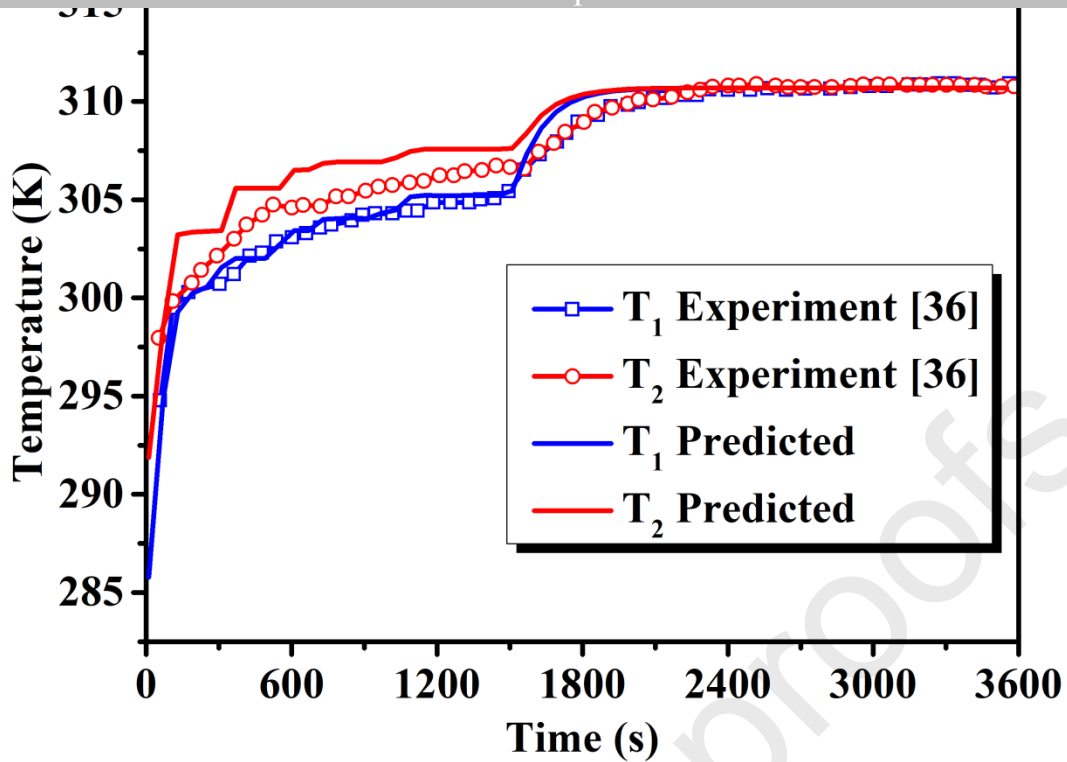
Fig. 4. The comparison between the present simulation and experimental test in reference [36].

4. Results and discussion

The melting process of LTES under periodic heat source is affected by the fluctuating characteristics of the heat sources, and the thermal resistance of both the PCM side and heat source side. Therefore, the effects of period and amplitude of a periodic heat source are firstly comprehensively investigated. Then a comparison of the charging process between the pure PCM and nano-PCM (composite PCM with metal nano-particle) is conducted in order to evaluate the effects of the thermal resistance of PCM side, considering the low thermal conductivity of pure PCM. Finally, the charging process of LTES, under different heat transfer coefficients of heat source, is analysed to illustrate the effects of the thermal resistance of the heat source side.

4.1 Analysis of different fluctuating period and amplitude

In this section, the heat transfer coefficient of the fluctuating heat source is set as h_f=90 W/(m² K) and the pure PCM is integrated with LTES. The contour of the total melting time of LTES under periodic heat source with different period

and amplitude are depicted in **Fig. 5**. Although the overall trend of total melting time decreases from 48.7 minutes to

36.1 minutes with an increase of the period and amplitude, the period and amplitude of fluctuating heat source have

different effects on the total melting time of LTES. In detail, when the period of fluctuating heat source is relatively

small, i.e., lower than 20 minutes, the amplitude almost does not affect the total melting time of LTES. With the period

augmenting, it can be found that the total melting time shortens as the amplitude of periodic heat source rises, that is,

the larger amplitude leads to promotion effects on the melting process of the shell-and-tube LTES. As for the effects of

the period for a periodic heat source, it can be found that the total melting time of LTES reveals a descending trend with

the increase of period at any certain amplitude, and the results illustrate that the periodic heat source with a larger period

can accelerate the melting process of LTES.
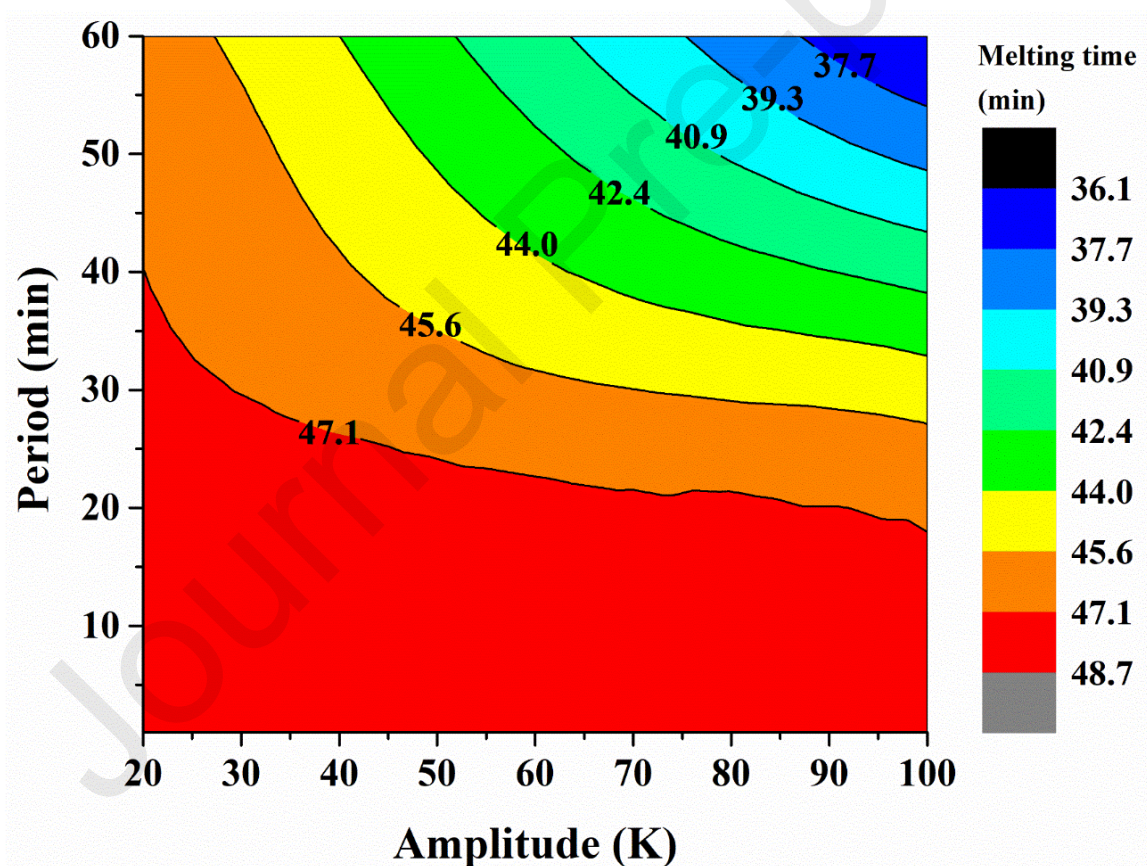
Fig. 5. The contour of total melting time under fluctuating heat source with different periods and

amplitudes.

The more obvious variation trend of the melting time with periods and amplitudes is shown in **Fig. 6**. When the

amplitude of periodic heat source is fixed at A=20 K, the total melting time changes from 48.3 minutes to 47.3 minutes while the period increases from 1 minute to 15 minutes and the variation trend is similar to the cases of A=60 K and 100 K. When the period continue to increase to 60 minutes, the total melting time decreases to 46.3 minutes, which is only 4.5% shorter than that of P=1 minute. However, that is not the case for A=60 K and 100 K. It can be seen from **Fig. 6** that the difference of total melting time between the cases with a small and large period is enlarged with the increase of the amplitude. In contrast, the total melting time of P=60 minutes is 36.1 minutes while it is 48.7 minutes for P=1 minute. Therefore the result at P=60 minutes is 25.7% shorter than that of P=1 minute. Based on the previous analysis, the effects of period and amplitude for fluctuating heat sources can be concluded as the following: the fluctuating heat source with small periods has little effect on the melting process of LTES whether the fluctuating amplitude is small or large. Meanwhile, the fluctuating heat sources with large periods and small amplitudes have a relatively minor influence on the melting process of LTES while the cases with large periods and amplitudes considerably speed up the melting process.
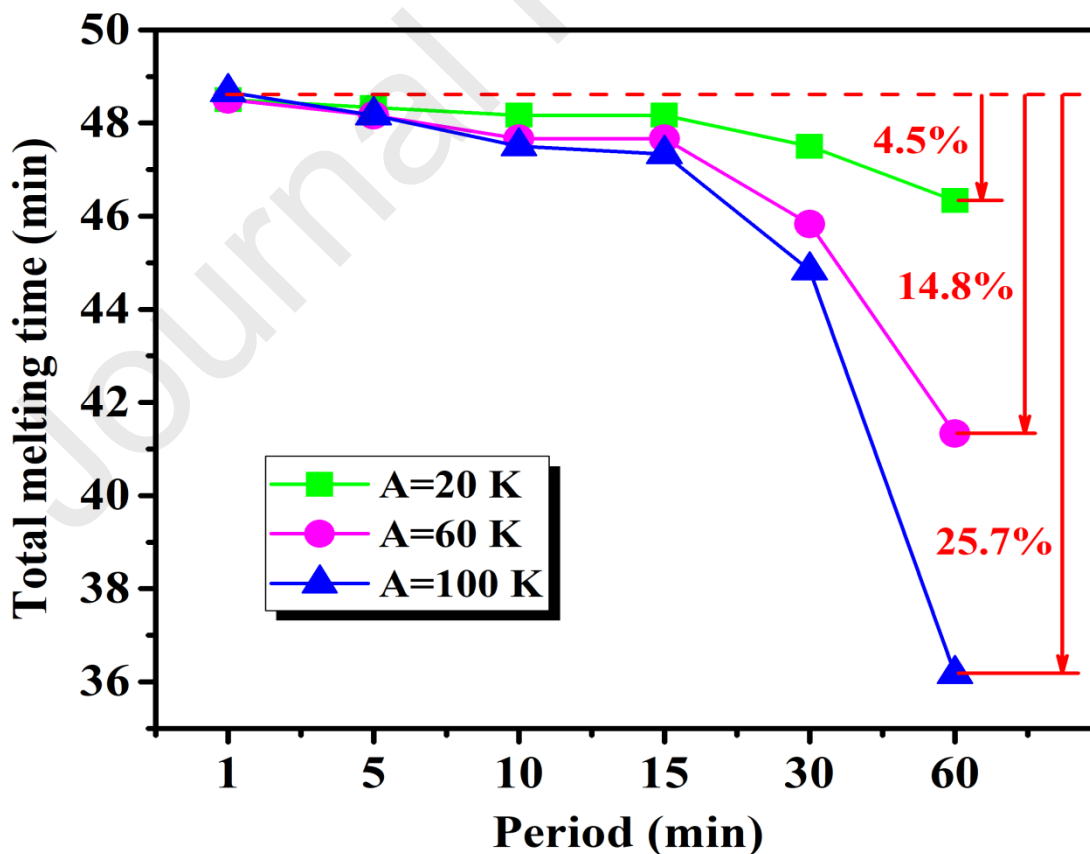
To further reveal the melting process of LTES under fluctuating heat source with different period and amplitude, the evolution of liquid volume fraction of LTES is analysed as shown in **Fig. 7**. The liquid volume fraction indicates almost the same variation trend for a different period in **Fig. 7** (a) when the fluctuating amplitude A is only 20 K. Due to the small amplitude of these fluctuating heat source, the amount of heat flux transferred to the LTES from the fluctuating heat source also fluctuates with small amplitude although their periods vary from 1 minute to 60 minutes. This results in the heat flux for different cases being slightly different from each other during every unit time-lag (e.g. 1 minute), i.e. the evolution of temperature field for these cases is quite similar. **Fig. 8** presents the contour of temperature and velocity of LTES at different times with A=20 K. The contours of temperature and velocity of LTES are almost consistent with each other for a fluctuating heat source with different periods at the moment of t=5 minutes. With the time elapsing, the temperature of LTES increases and the velocity first strengthens and then recedes, but the contours of temperature and velocity for different cases with A=20 K still remain reasonably comparable. Overall, the similar melting process has demonstrated that the period of fluctuating heat source has a limited effect on the total melting time of LTES when the fluctuating amplitude is small.

(a) Fluctuating amplitude A=20 K   (b) Fluctuating amplitude A=100 K
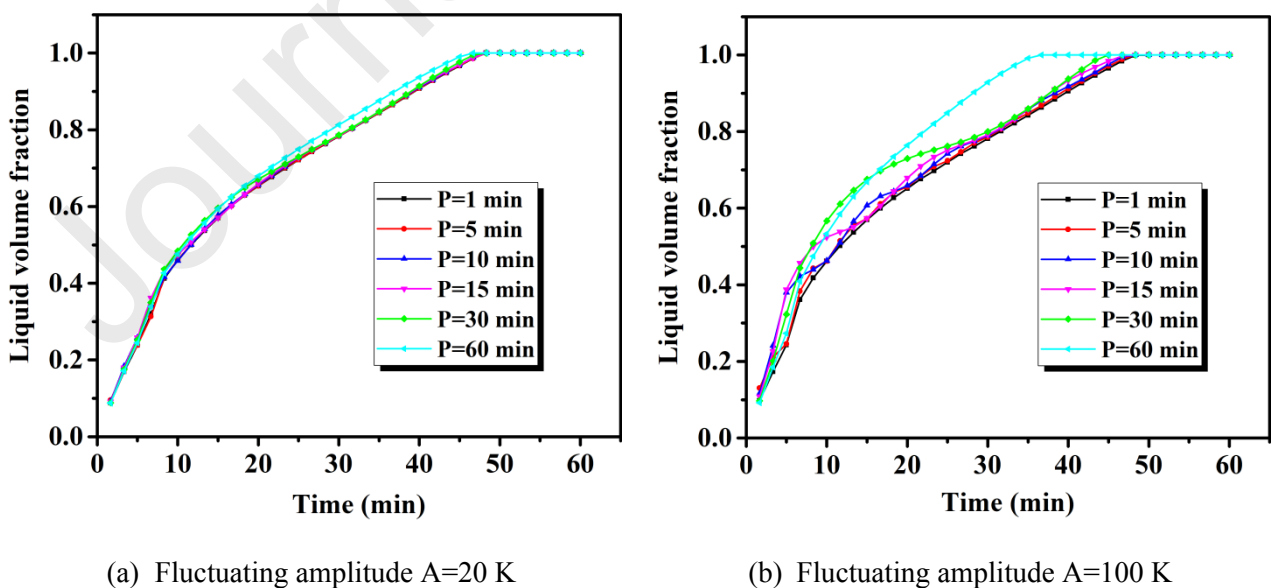
Fig. 7. The evolution of liquid volume fraction of pure PCM under different fluctuating periods.

17

Nevertheless, when the amplitude of fluctuating heat source increases to A=100 K, the difference of the melting process of LTES changes significantly as shown in **Fig. 7** (b). It can be seen that the melting rate of LTES consistently increases with the enlargement of the fluctuating period, particularly for the fluctuating heat source with a larger period (i.e. P=30, 60 minutes). Due to the large amplitude of the fluctuating heat source, the total heat absorbed by the LTES is quite significant for large-period fluctuating heat sources in the earlier stage of the melting process (t<20 min), which significantly enhances the melting process of LTES and leads to a larger liquid volume fraction. In return, the natural convection existing in the liquid PCM improves the meting rate of LTES. As for the wavelike trend of liquid volume fraction, this occurs because the LTES can absorb much more heat from the fluctuating heat source during every first-half period than that of every second-half period, resulting in the liquid volume fraction increasing quickly in the first half period and then increasing at a much slower rate in the second half period for fluctuating heat sources, i.e., the evolution of liquid volume fraction presents a wavelike rise trend due to the fluctuation of the heat source.
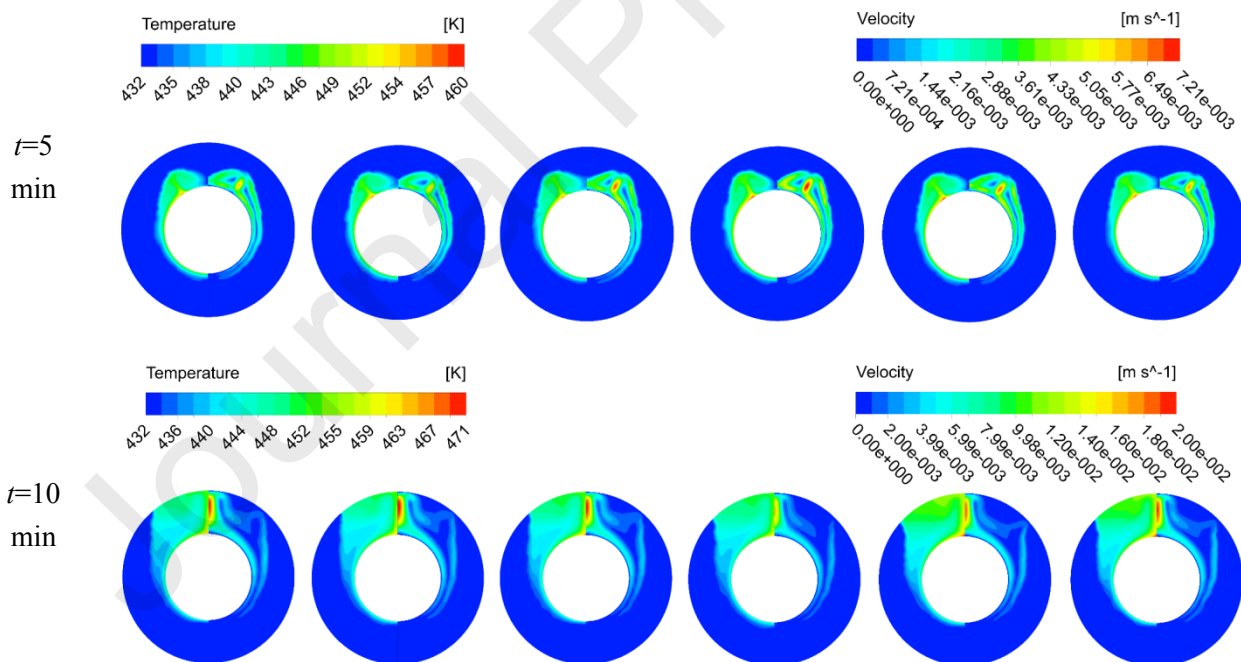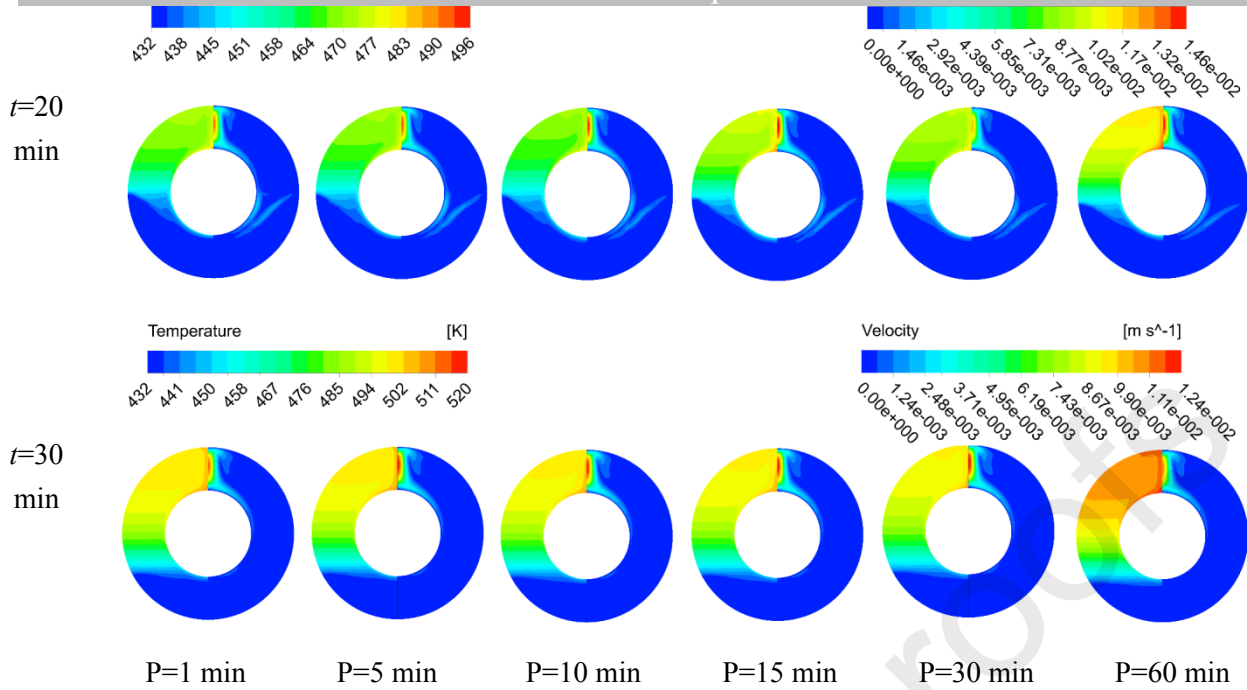
Fig. 8. The contour of PCM temperature (left semi-circle) and velocity (right semi-circle) under different

fluctuating periods with A=20 K.

Fig. 9 illustrates the heat storage capacity of LTES under a fluctuating heat source with different periods and amplitudes

at the end of the charging process. It is clear that the overall trend of the heat stored by PCM declines with the increase

of period and amplitude. However, it can be demonstrated that the variation of the heat stored by PCM is not sensitive

to the fluctuating heat source with small amplitude and period. For example, when the fluctuating period is smaller than

P=20 min and the fluctuating amplitude is lower than A= 50 K, the isolines are much sparser than other areas in the

contour map. With the augmentation of the fluctuating period and amplitude, the heat stored by PCM declines faster.

The clear variation trend of the heat stored by PCM under different fluctuating periods and amplitudes is illuminated in

Fig. 10.
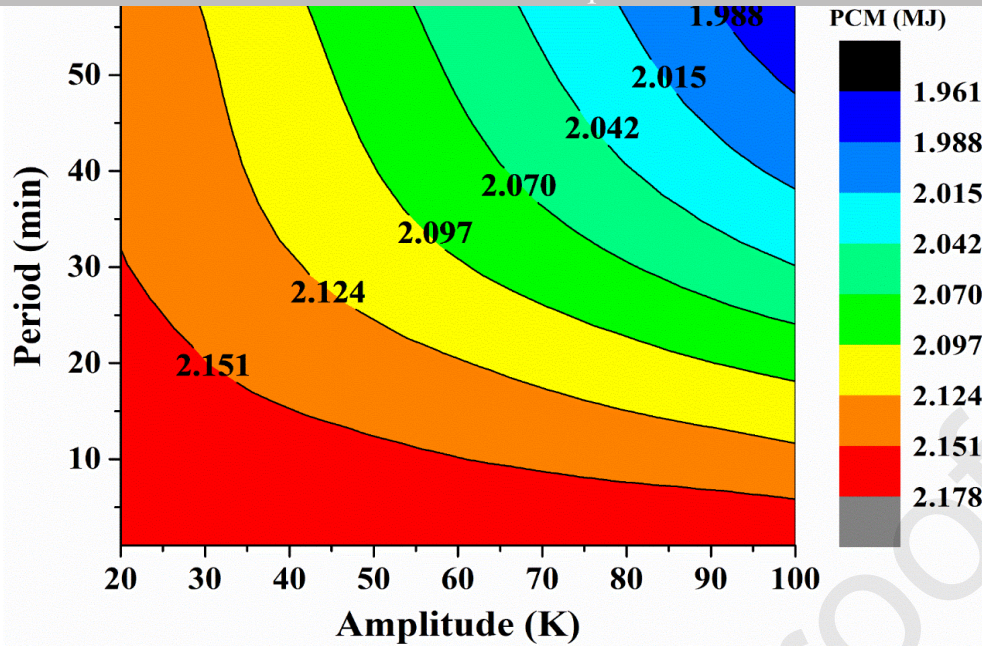
Fig. 9. The contour of heat stored by PCM under fluctuating heat source with different periods and

amplitudes.

When the fluctuating amplitude is fixed at A=20 K, the heat stored by PCM indicates a very slight reduction (1.7%) as

the fluctuating period increases from P=1 minute to P=60 minute. As previously analysed, the fluctuating heat source

with small periods has limited effect on the melting process of LTES whether the fluctuating amplitude is small or large,

that is, the evolution of temperature field of LTES is almost consistent in all cases as depicted in **Fig. 8**. Therefore, the

heat flux between the LTES and fluctuating heat source is also consistent in all cases although the fluctuating period

varies from 1 minute to 60 minutes during the whole melting process. When the fluctuating amplitude rises to A=60 K,

the reduction percentage also increases to 5.6% with an increase of the fluctuating period. When the fluctuating

amplitude is as large as A=100 K, the reduction percentage of the heat stored by PCM becomes as significant as 9.8%

with the fluctuating period increasing from 1 minute to 60 minutes. Similarly, the total melting time substantially

decreases with the increase of the fluctuating period when the amplitude is A=100 K, and the higher average temperature

of PCM is produced as a result of the faster melting process, which narrows down the temperature difference between

the PCM and fluctuating heat source and naturally brings about a reduced amount of heat stored by PCM.
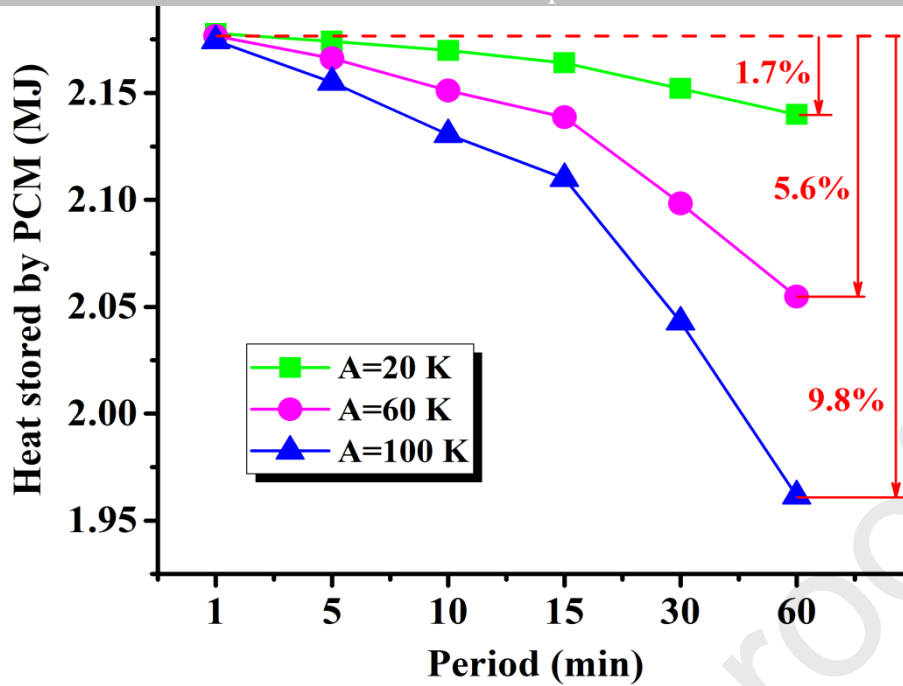
Fig. 10. Variation of heat stored by pure PCM under fluctuating heat source.

4.2 Effects of PCM thermal conductivity

In **Section 4.1**, the melting process of LTES using pure PCM is investigated under the fluctuating heat source. However, the melting process of LTES is significantly affected by the thermal conductivity of PCM. Due to the low thermal conductivity of the pure PCM, the melting process of LTES using composite PCM with Al_2O_3 nanoparticles is analysed, under fluctuating heat source, with different periods and amplitudes. The heat transfer coefficient of the fluctuating heat source is set as h_f=90 W/ (m^2 K). **Fig. 11** shows the total melting time of composite PCM with nanoparticle concentration of 5% under the fluctuating heat source. Due to the existance of Al_2O_3 nanoparticles, the thermal conductivity of PCM is improved from 0.88 W/(m K) to 1.20 W/(m K), that is, a percentage of 36.4%. Therefore, the LTES integrating composite PCM indicates a faster melting process compared to the pure PCM in any fluctuating heat source scenarios. It can be observed that the improvement in the thermal conductivity has not changed the overall trend of the total melting time of composite PCM compared, with pure PCM, under the fluctuating heat source, i.e., the total melting time decreases with the increase of period and amplitude. For LTES using composite PCM, it is worth noting that the total

melting time remains insensitive to the period and amplitude when they are within a short range.
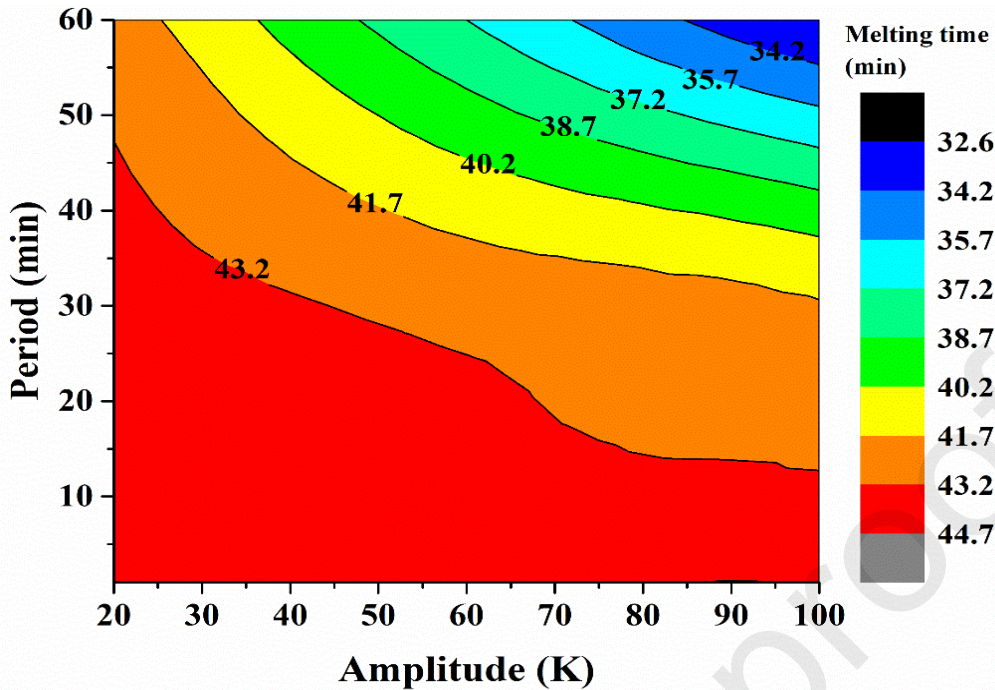
Fig. 11. The contour of total melting time of composite PCM with Al_2O_3 concentration of 5% under the

fluctuating heat source.

Detailed evidence of this situation is shown in **Fig. 12**. When the amplitude is fixed at A=20 K, the total melting

decreases by 4.9% when the period increases from P=1 minute to P=60 minutes, while the corresponding value is 4.5%

for the pure PCM as shown in **Fig. 6**. With an increase of the fixed amplitude, the total melting time of the composite

PCM decreases by 16.8% for A=60 K and 26.9% for A=100, while the results are 14.8% and 25.7 for pure PCM,

respectively. The above results can be explained because the higher thermal conductivity can improve the heat transfer

process inside the entire PCM. In detail, when the period and amplitude of the fluctuating heat source is large, the

melting rate is large at the early stage, as previously analysed. The higher thermal conductivity of the composite PCM

further improves the melting rate and the natural convection in liquid volume fraction is also enhanced. Additionally,

the higher thermal conductivity improves the heat transfer rate inside the composite PCM and leads to more uniform

temperature distribution in the late melting process, which is helpful for the melting of the left composite PCM in the

final stage of melting process.
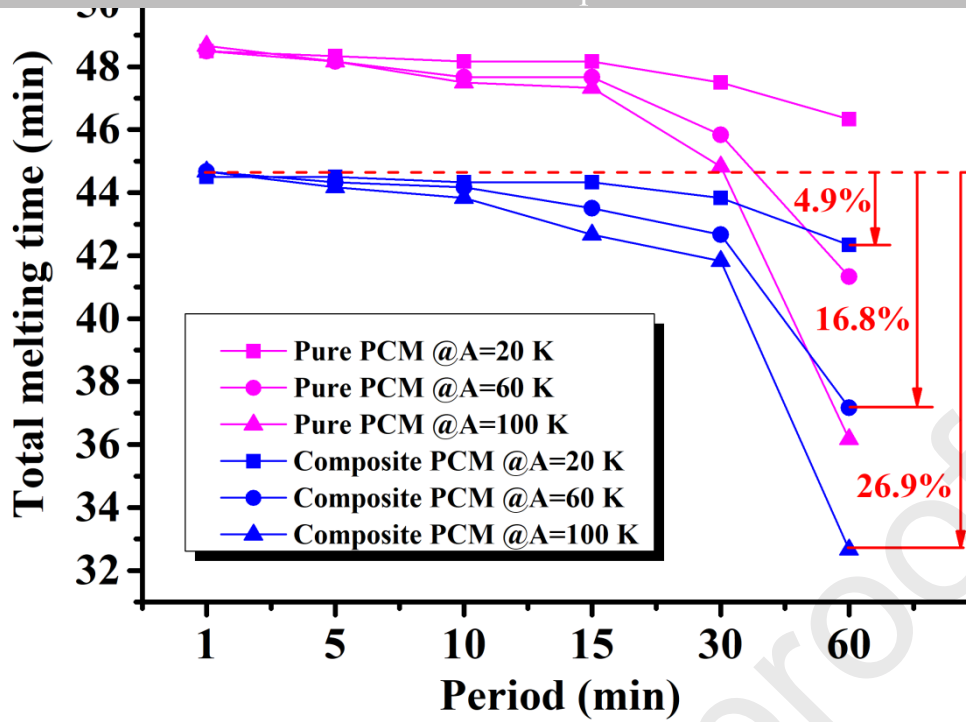
Fig. 12. Variation of total melting time of composite PCM with Al_2O_3 concentration of 5% under the

fluctuating heat source.

Results relevant to the energy storage capacity of LTES using composite PCM under fluctuating heat source can be seen

in **Fig. 13**. The overall trend of the heat stored by composite PCM is the same as that of the pure PCM and this can be

observed in **Fig. 9**, that is, the amount of heat stored by the composite PCM decreases as the period and amplitude of

the fluctuating heat source increase.. However, the amount of heat stored by the composite PCM is very similar

compared with that of the pure PCM. Additionally, the existing of Al_2O_3 nanoparticles have not changed the effects of

the period and amplitude of fluctuating heat source on the heat storage capacity. In summary, the increase of the PCM

thermal conductivity has limited impact on the heat storage capacity.
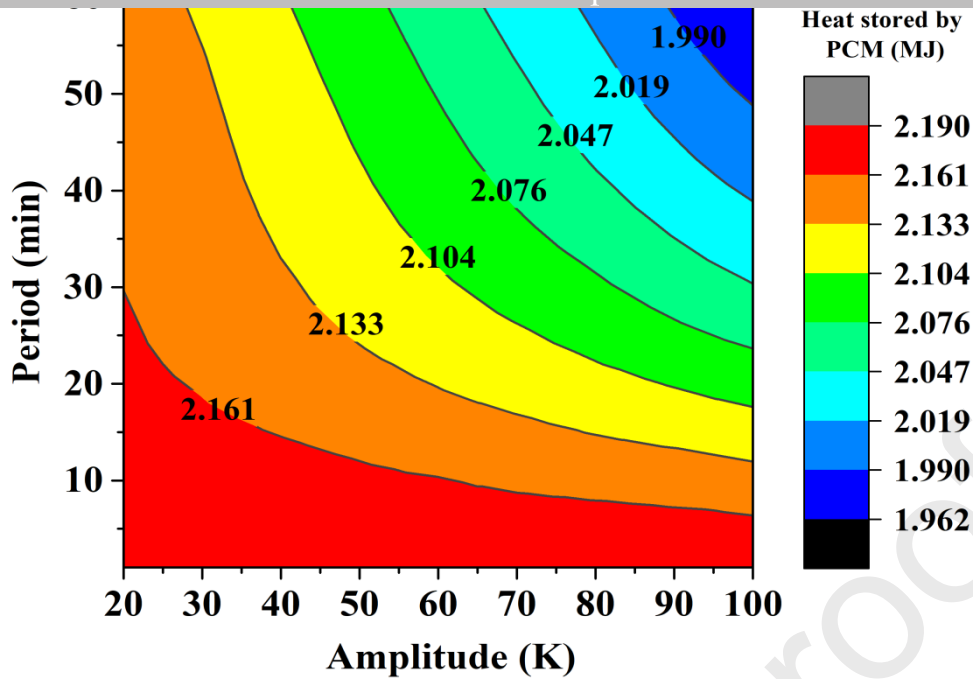
Fig. 13. The contour of heat stored by composite PCM with a concentration of 5% under fluctuating heat

source.

Detailed results and trends, with respect to the heat storage capacity of composite PCM compared to pure PCM, is

depicted in **Fig. 14**. At any fixed amplitude, it can be observed that the heat storage capacity decreases with an increase

of the period for both the pure and composite PCM, and minor improvement in heat storage capacity is obtained by

using composite PCM irrespective of the period size. The addition of nanoparticles can improve the heat transfer rate

inside the composite PCM and speed up the process of heat transferring from a high-temperature location to a low-

temperature location, leading to a more uniform temperature field and a lower average temperature of PCM domain.

Therefore, the temperature difference between the PCM and fluctuating heat source is narrowed down to some extent,

which is helpful for improving the heat flux during the charging process. However, it should be noted that introducing

nanoparticles also has diminished the latent heat and specific heat capacity of the composite PCM, which are the

important factors for heat storage capacity. The comprehensive effects result in a slight increase in heat storage capacity

when comparing the composite PCM with the pure PCM. Based on above analysis about the effects of nanoparticles on

the melting time and heat storage capacity of LTES using a composite PCM, it can be concluded that the increase of the

24

PCM thermal conductivity significantly reduces the total melting time, but shows very limited impact on the heat storage capacity of LTES using a composite PCM.
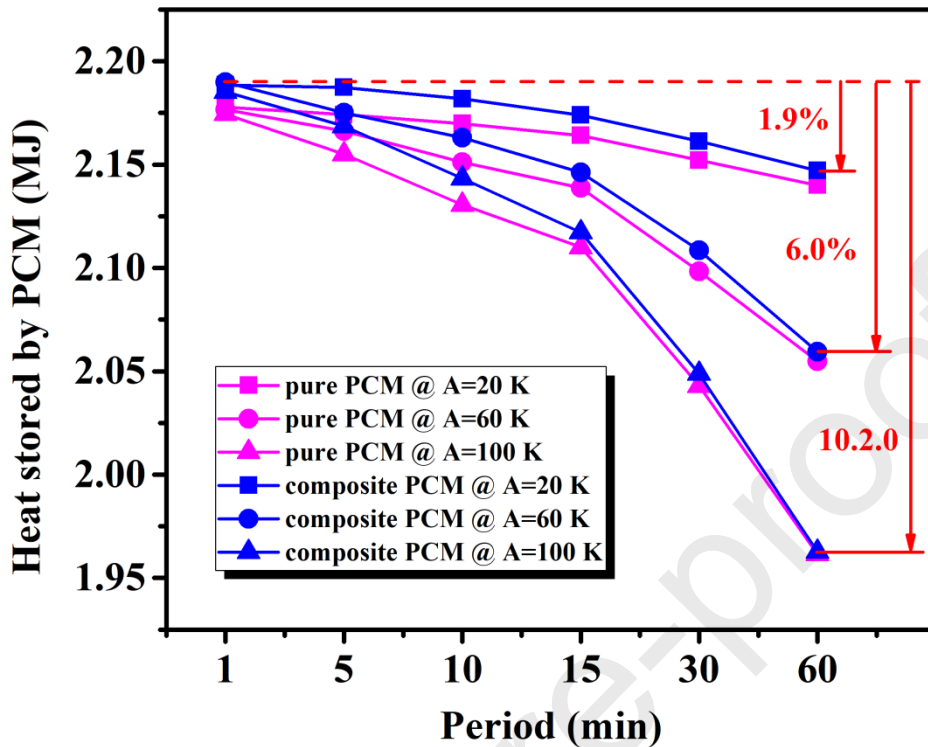
Fig. 14. Comparison of heat storage capacity between pure and composite PCM under fluctuating heat source with different periods and amplitudes.

4.3 Effects of heat transfer coefficient of heat source

Apart from the thermal resistance of the PCM side, the thermal resistance of the heat source side also plays an important role in determining the melting process of LTES. In this section, the heat transfer coefficient of fluctuating heat source increases from 90 W/(m² K) to 180 W/(m² K), and the effects of the heat transfer coefficient of fluctuating heat source on the melting process of LTES using pure PCM is investigated under different periods and amplitudes. **Fig. 15** indicates the contour of total melting time with h_f=180 W/(m² K) under the fluctuating heat source. Overall, the total melting time of the PCM is substantially reduced due to the larger heat transfer coefficient of a fluctuating heat source with any period and amplitude. The larger heat transfer coefficient results in higher heat flux between the fluctuating heat source and PCM, reasonably shortening the total melting time of the PCM. It is important to note that the increase of heat transfer

coefficient has changed the effects of period and amplitude on the total melting time of the PCM. In detail, it can be found that the larger heat transfer coefficient has narrowed the insensitive scope for the total melting time, that is the difference of total melting time between the small-period fluctuating heat sources has been enlarged. Meanwhile, compared with the case of h_f=90 W/(m² K) shown in **Fig. 5**, the increase of heat transfer coefficient amplified the effects of amplitude when the period of the fluctuating heat source is fixed, especially if the period is relatively small (P<20 min). For example, the total melting time decreases by 6.5% with the amplitude rising from 20 K to 100 K when the period is fixed at P=15 min, whilst the corresponding value is only 1.7% for the case of h_f=90 W/(m² K).
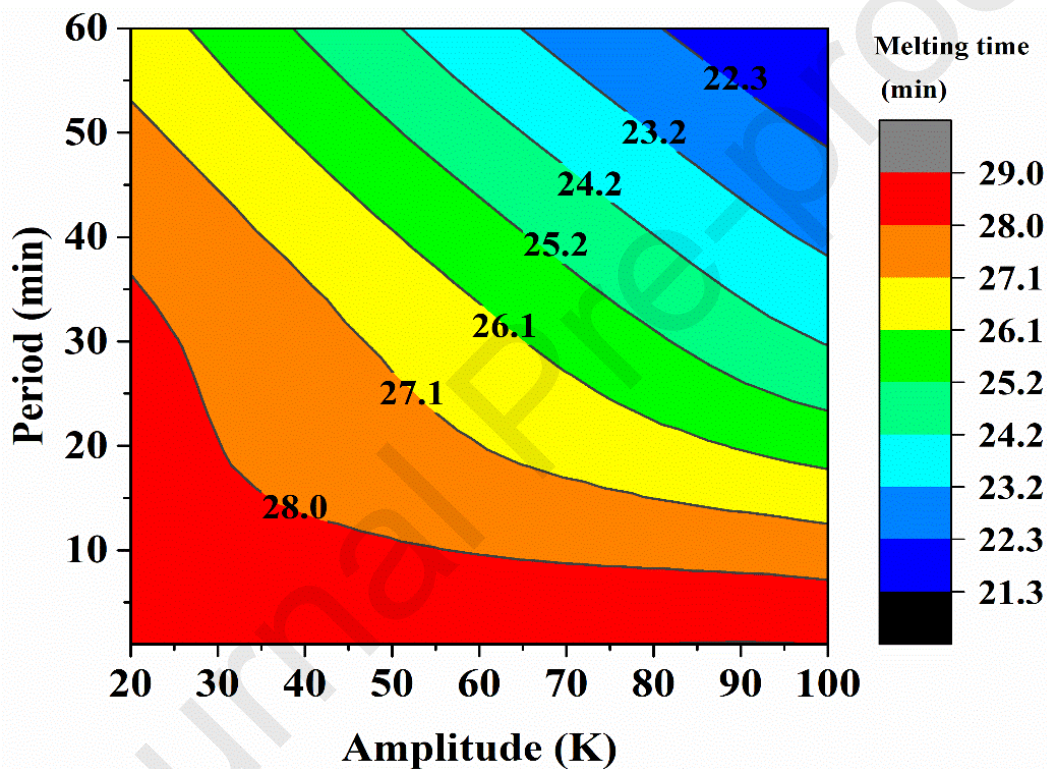
Fig. 15. The contour of total melting time of PCM with h_f=180 W/(m² K) under fluctuating heat source.

Fig. 16 shows the variation of total melting time of a PCM with period at a fixed fluctuating amplitude when the heat transfer coefficient is set as h_f=180 W/(m² K). The total melting time decreases significantly when the period increases from 1 minute to 30 minutes at any fixed amplitude, especially at A=60 K and A=100 K. The results demonstrate that the larger heat transfer coefficient has enlarged the difference of total melting time of cases with small periods compared with the case of h_f=90 W/(m² K), asshown in **Fig. 6**, and the difference continues to increase as the amplitude increases.

This is because the larger heat transfer coefficient brings about higher heat flux in each unit of time for cases with different periods at a fixed amplitude, as well as the larger difference of heat flux between the cases with smaller periods such as P=1 minute and larger periods such as P=15 minutes during each unit of time. This then leads to a larger difference of total meting time between the cases with small periods compared with the results of h_f=90 W/(m^2 K). Additionally the larger heat transfer coefficient enlarges the difference of total melting between the case of P=1 minute and P=60 minutes compared with h_f=90 W/(m^2 K) case. When the amplitude of the fluctuating heat source is fixed at A= 20K, the total melting time decreases by 7.5% while it is only 4.5% for the case of h_f=90 W/(m^2 K). With the fixed amplitude increasing to A=60 K and 100 K, the decreased value in percentage terms is 17.1% and 26.4% when the period rises from P=1 minute to P=60 minute, while the corresponding values are 14.8% and 25.7% for the case of h_f=90 W/(m^2 K), respectively.
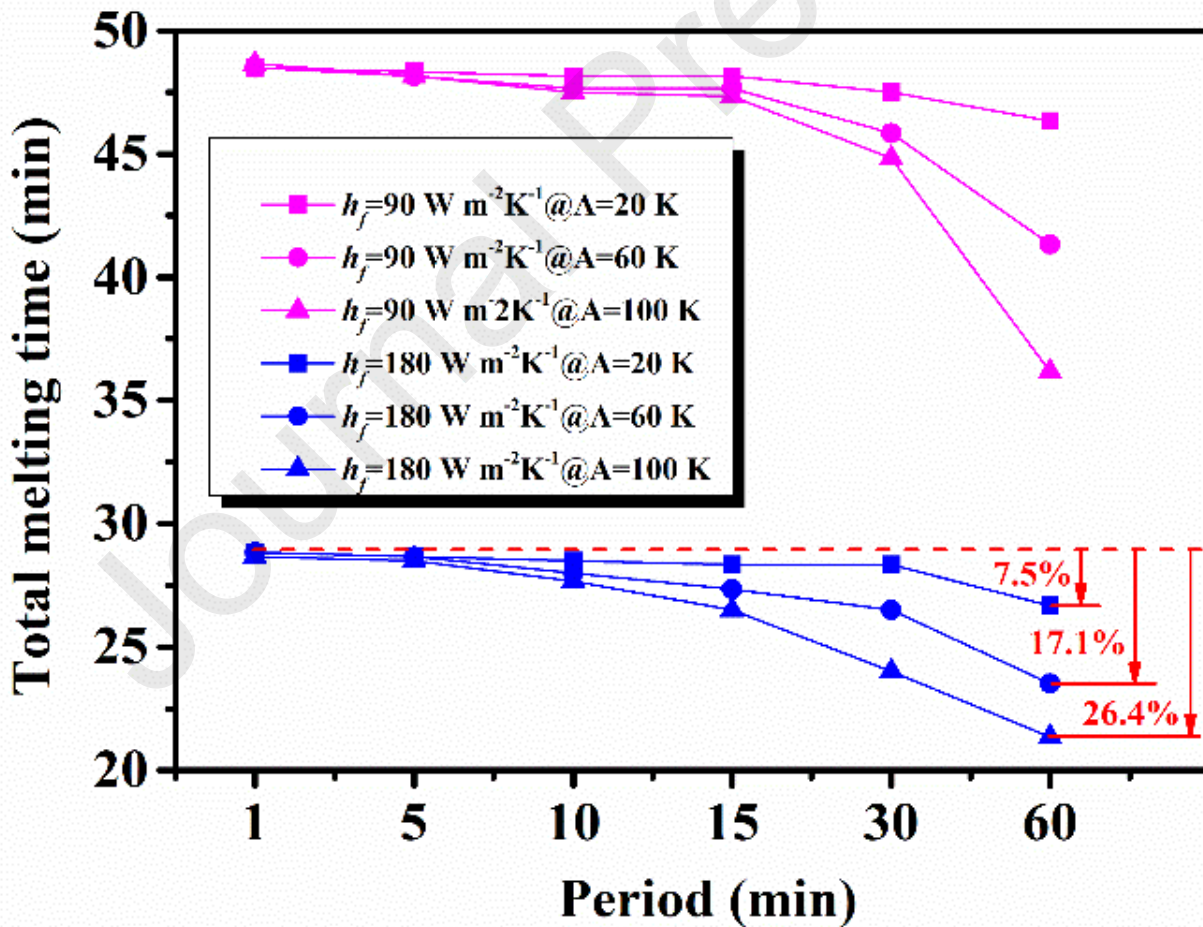
Fig. 16. Variation of total melting time of PCM with h_f =180 W/(m^2 K) under fluctuating heat source.

Fig. 17 illustrates the contour of heat stored by the PCM under a fluctuating heat source when the heat transfer coefficient is set as h_f=180 W/(m² K). Although the heat transfer coefficient increases from 90 W/(m² K) to 180 W/(m² K), the heat stored by the PCM still maintains the overall trend i.e. it declines with the enlargement of the period and amplitude of the fluctuating heat source. However, the denser contour lines in **Fig. 17** indicated that the increased heat transfer coefficient has amplified the sensibility of heat storage capacity to the period and amplitude of the fluctuating heat source, that is to say, the change of period and amplitude result in more significant effects on the heat storage capacity. Even the period and amplitude are located at the left bottom of the contour figure, and it is particularly obvious for the small-period fluctuating heat source (P<20 minutes) with any amplitude.
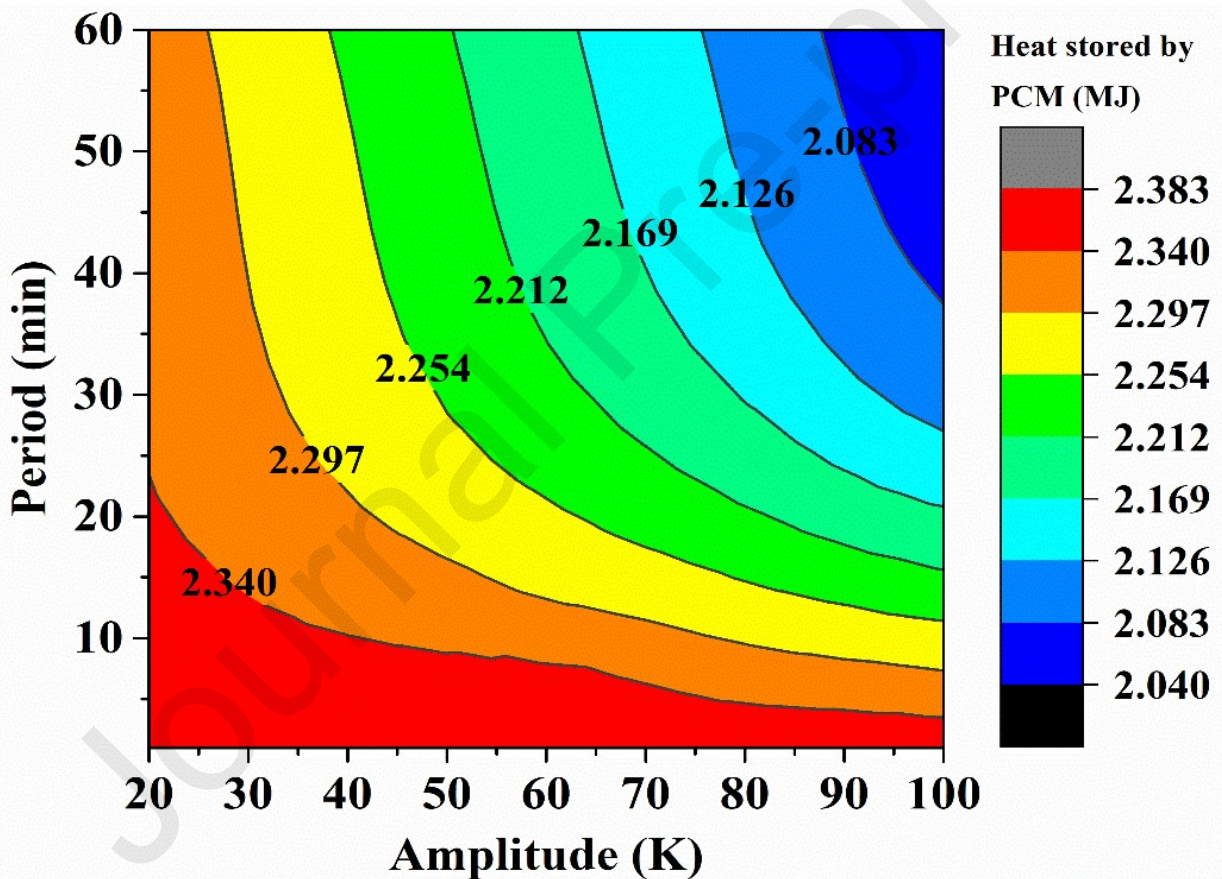
Fig. 17. The contour of heat stored by PCM with h_f=180 W/(m² K) under the fluctuating heat source.

Fig. 18 indicates the variation of heat stored by a PCM across range of periods when the heat transfer coefficient is set as h_f=180 W/(m² K). It can be seen that the heat stored by PCM declines, in a more dramatic trend, when the period

increases from P = 1 minute to P = 10 minutes, than the case of h_f = 90 W/(m² K). Furthermore, the trend is more obvious

when the fixed amplitude increases from A=20 K to A=100 K. In addition, at any fixed amplitude of the fluctuating heat

source, the difference of heat storage capacity between the small-period and large-period heat source increases, and the

difference gets bigger with the increase of fixed amplitude. In detail, the heat storage capacity of PCM decreases by

2.8%, 8.3% and 13.9% when the period of the fluctuating heat source rises from P=1 minute to P=60 minute at the fixed

amplitude of A=20 K, 60 K and 100 K, respectively. As a comparison, the corresponding decrease percentage is 1.7%,

5.6% and 9.8% for the case of h_f=90 W/(m² K).
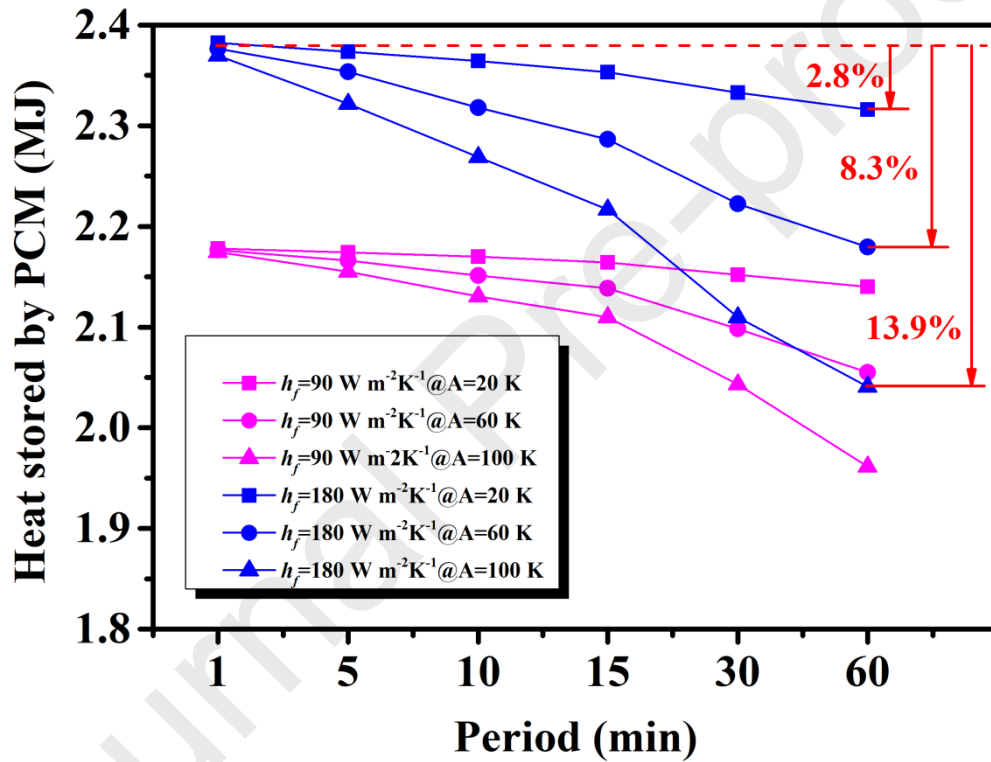
Fig. 18. Variation of heat stored by PCM with h_f =180 W/(m² K) under fluctuating heat source.

5. Conclusions

In this study, the melting process of a shell-and-tube LTES unit under fluctuating thermal conditions has been studied

to provide valuable information which can be used in the design and optimization of LTES and address the fluctuation

issues associated with heat sources such as the solar energy, geothermal, industrial processes. The crucial factors, include

the period and amplitude of fluctuating heat source, the thermal conductivity of the PCM, and the heat transfer

coefficient of fluctuating heat source, are comprehensively investigated. The main conclusions drawn as follows.

(1) The overall trend of total melting time and heat storage capacity decreases with an increase of period and amplitude. When the period of the fluctuating heat source is low (P<20 minutes), the total melting time and heat storage capacity are not sensitive to the variation of amplitude. However the fluctuating heat source with large period and amplitude significantly reduce the total melting time and heat storage capacity. For example, the total melting time and heat storage capacity only decreases by 4.5% and 1.7% when the period increases from 1minute to 60 minutes at a fixed amplitude of A=20 K, whilst the corresponding values are 25.7% and 9.8% at a fixed amplitude of A=100 K.

(2) Although the composite PCM has not changed the overall trend of total melting time with variations to the period and amplitude, compared to the pure PCM, the higher thermal conductivity of the composite PCM results in the total melting time being more sensitive to the period and amplitude when they are large. For example, the total melting time decreases by 4.5% and 25.7% with the period increasing from 1 minute to 60 minutes at the fixed amplitude of A=20 K and A=100 K respectively, while the corresponding values are 4.9% and 26.9% for pure PCM.

(3) An increased heat transfer coefficient has also narrowed the insensitivity range for the total melting time, and enlarged the effects of amplitude when the period is fixed, particularly when the period is relatively small (P<20 min). Additionally, the difference of heat storage capacity results between the small-period and large-period heat source increases at any fixed amplitude of fluctuating heat source, and the difference increases further with an increase of fixed amplitude.

Acknowledgements

Reference

[1] F. Dal Magro, M. Jimenez-Arreola, A. Romagnoli, Improving energy recovery efficiency by retrofitting a PCM-based technology to an ORC system operating under thermal power fluctuations, Applied Energy, 208 (2017) 972-985.

[2] M. Jiménez-Arreola, R. Pili, F. Dal Magro, C. Wieland, S. Rajoo, A. Romagnoli, Thermal power fluctuations in waste heat to power systems: An overview on the challenges and current solutions, Applied Thermal Engineering, 134 (2018) 576-584.

[3] J. Pereira da Cunha, P. Eames, Thermal energy storage for low and medium temperature applications using phase change materials – A review, Applied Energy, 177 (2016) 227-238.

[4] L. Shi, G. Shu, H. Tian, S. Deng, A review of modified Organic Rankine cycles (ORCs) for internal combustion engine waste heat recovery (ICE-WHR), Renewable and Sustainable Energy Reviews, 92 (2018) 95-110.

[5] Y. Lu, A.P. Roskilly, X. Yu, K. Tang, L. Jiang, A. Smallbone, L. Chen, Y. Wang, Parametric study for small scale engine coolant and exhaust heat recovery system using different Organic Rankine cycle layouts, Applied Thermal Engineering, 127 (2017) 1252-1266.

[6] F. Dal Magro, A. Meneghetti, G. Nardin, S. Savino, Enhancing energy recovery in the steel industry: Matching continuous charge with off-gas variability smoothing, Energy Conversion and Management, 104 (2015) 78-89.

[7] F. Dal Magro, S. Savino, A. Meneghetti, G. Nardin, Coupling waste heat extraction by phase change materials with superheated steam generation in the steel industry, Energy, 137 (2017) 1107-1118.

[8] B.-R. Fu, S.-W. Hsu, Y.-R. Lee, J.-C. Hsieh, C.-M. Chang, C.-H. Liu, Effect of off-design heat source temperature on heat transfer characteristics and system performance of a 250-kW organic Rankine cycle system, Applied Thermal Engineering, 70 (2014) 7-12.

[9] G. Shu, M. Zhao, H. Tian, H. Wei, X. Liang, Y. Huo, W. Zhu, Experimental investigation on thermal OS/ORC (Oil Storage/Organic Rankine Cycle) system for waste heat recovery from diesel engine, Energy, 107 (2016) 693-706.

[10] H. Jafari Mosleh, R. Ahmadi, Linear parabolic trough solar power plant assisted with latent thermal energy storage system: A dynamic simulation, Applied Thermal Engineering, 161 (2019) 114204.

[11] R. Jacob, M. Belusko, A. Inés Fernández, L.F. Cabeza, W. Saman, F. Bruno, Embodied energy and cost of high temperature thermal energy storage systems for use with concentrated solar power plants, Applied Energy, 180 (2016) 586-597.

[12] S. Li, H. Ma, W. Li, Dynamic performance analysis of solar organic Rankine cycle with thermal energy storage, Applied Thermal Engineering, 129 (2018) 155-164.

[13] G. Nardin, A. Meneghetti, F. Dal Magro, N. Benedetti, PCM-based energy recovery from electric arc furnaces, Applied Energy, 136 (2014) 947-955.

thermal energy storage for engine waste heat recovery, Energy, 170 (2019) 1098-1112.

[15] Z. Li, Z.-G. Wu, Analysis of HTFs, PCMs and fins effects on the thermal performance of shell–tube thermal energy storage units, Solar Energy, 122 (2015) 382-395.

[16] Y.B. Tao, V.P. Carey, Effects of PCM thermophysical properties on thermal storage performance of a shell-and-tube latent heat storage unit, Applied Energy, 179 (2016) 203-210.

[17] G.-S. Han, H.-S. Ding, Y. Huang, L.-G. Tong, Y.-L. Ding, A comparative study on the performances of different shell-and-tube type latent heat thermal energy storage units including the effects of natural convection, International Communications in Heat and Mass Transfer, 88 (2017) 228-235.

[18] A. Ebrahimi, M.J. Hosseini, A.A. Ranjbar, M. Rahimi, R. Bahrampoury, Melting process investigation of phase change materials in a shell and tube heat exchanger enhanced with heat pipe, Renewable Energy, 138 (2019) 378-394.

[19] Y.H. Diao, L.L. Yin, Z.Y. Wang, Y.H. Zhao, L. Liang, F.W. Bai, Numerical analysis of heat transfer characteristics for air in a latent heat thermal energy storage using flat miniature heat pipe arrays, Applied Thermal Engineering, 162 (2019) 114247.

[20] D. Han, B. Guene Lougou, Y. Xu, Y. Shuai, X. Huang, Thermal properties characterization of chloride salts/nanoparticles composite phase change material for high-temperature thermal energy storage, Applied Energy, 264 (2020) 114674.

[21] B. Buonomo, H. Celik, D. Ercole, O. Manca, M. Mobedi, Numerical study on latent thermal energy storage systems with aluminum foam in local thermal equilibrium, Applied Thermal Engineering, 159 (2019) 113980.

[22] Y.B. Tao, Y.L. He, Numerical study on performance enhancement of shell-and-tube latent heat storage unit, International Communications in Heat and Mass Transfer, 67 (2015) 147-152.

[23] Y.B. Tao, Y.L. He, Numerical study on thermal energy storage performance of phase change material under non-steady-state inlet boundary, Applied Energy, 88 (2011) 4172-4179.

[24] H.J. Xu, C.Y. Zhao, Thermal performance of cascaded thermal storage with phase-change materials (PCMs). Part II: Unsteady cases, International Journal of Heat and Mass Transfer, 106 (2017) 945-957.

[25] Y. Huo, J. Zong, Z. Rao, The investigations on the heat transfer in thermal energy storage with time-dependent heat flux for power plants, Energy, 175 (2019) 1209-1221.

[26] Z. Li, X. Yu, L. Wang, Y. Lu, R. Huang, J. Chang, R. Jiang, Effects of fluctuating thermal sources on a shell-and-tube latent thermal energy storage during charging process, Energy, 199 (2020) 117400.

[27] J.M. Mahdi, H.I. Mohammed, E.T. Hashim, P. Talebizadehsardari, E.C. Nsofor, Solidification enhancement with multiple PCMs, cascaded metal foam and nanoparticles in the shell-and-tube energy storage system, Applied Energy, 257 (2020) 113993.

[28] R.P. Singh, H. Xu, S.C. Kaushik, D. Rakshit, A. Romagnoli, Charging performance evaluation of finned conical thermal storage system encapsulated with nano-enhanced phase change material, Applied Thermal Engineering, 151 (2019) 176-190.

[29] R.S. Vajjha, D.K. Das, Experimental determination of thermal conductivity of three nanofluids and development of new correlations, International Journal of Heat and Mass Transfer, 52 (2009) 4675-4682.

[30] and multi-PCM-tube heat exchanger, Journal of Energy Storage, 22 (2019) 88-97.

[31] Y.B. Tao, Y.L. He, Effects of natural convection on latent heat storage performance of salt in a horizontal concentric tube, Applied Energy, 143 (2015) 38-46.

[32] A.A. Al-Abidi, S. Mat, K. Sopian, M.Y. Sulaiman, A.T. Mohammad, Numerical study of PCM solidification in a triplex tube heat exchanger with internal and external fins, International Journal of Heat and Mass Transfer, 61 (2013) 684-695.

[33] S. Deng, C. Nie, G. Wei, W.-B. Ye, Improving the melting performance of a horizontal shell-tube latent-heat thermal energy storage unit using local enhanced finned tube, Energy and Buildings, 183 (2019) 161-173.

[34] M. Jiménez-Arreola, R. Pili, C. Wieland, A. Romagnoli, Analysis and comparison of dynamic behavior of heat exchangers for direct evaporation in ORC waste heat recovery applications from fluctuating sources, Applied Energy, 216 (2018) 724-740.

[35] M. Jiménez-Arreola, C. Wieland, A. Romagnoli, Direct vs indirect evaporation in Organic Rankine Cycle (ORC) systems: A comparison of the dynamic behavior for waste heat recovery of engine exhaust, Applied Energy, 242 (2019) 439-452.

[36] M. Lacroix, Numerical simulation of a shell and tube latent thermal energy storage unit, Solar Energy, 50 (1993) 357-367.